Article

The Role of Organosulfur Compounds in the Growth of PbS Quantum Dots

Martin R. McPhail, and Emily A. Weiss

Chem. Mater., **Just Accepted Manuscript** • DOI: 10.1021/cm4040819 • Publication Date (Web): 15 May 2014

The Role of Organosulfur Compounds in the Growth and Final Surface Chemistry of PbS Quantum Dots

*Martin R. McPhail and Emily A. Weiss**

Dept. of Chemistry, Northwestern University, Evanston, IL 60208-3113

*corresponding author. Email: e-weiss@northwestern.edu

ABSTRACT

This paper describes the mechanism by which reaction of sulfur with octadecene (ODE) induces a change in the shape of PbS quantum dots (QDs), synthesized from the S/ODE precursor and lead oleate, from cubic to hexapodal by altering the ligand chemistry of the growing QDs. ^{1}H-NMR and optical spectroscopies indicate that extended heating of sulfur and ODE at 180 °C produces a series of organosulfur compounds with optical transitions in the visible region, and that the binding of organosulfur ligands to the growing QD induces a preferential growth at the <100> faces (over the <111> faces), and therefore a hexapodal geometry for the particles. The study shows that S/ODE can be made a more reliable precursor by reducing the temperature and duration of the sulfur dissolution step, and that any metal sulfide QD synthesis using elemental sulfur heated to high temperatures should take steps to reduce the *in situ* yield of organosulfur byproducts by avoiding olefinic solvents.

INTRODUCTION

This paper describes the mechanisms by which the composition of the sulfur-1-octadecene (S/ODE) precursor modifies both the shape and surface chemistry of lead sulfide quantum dots (PbS QDs) produced using reaction mixtures of S/ODE and lead oleate. The S/ODE precursor is useful for the scalable synthesis of metal sulfide QDs because it is cheap, air-stable, and highly reactive with reducing agents. S/ODE has become a primary sulfur source for the CdS QD synthesis following the original report of Yu and Peng[1]; dozens of reports detail its use to prepare CdS QDs and core/shell particles.[2-14] More recently, S/ODE has become a popular precursor for PbS QD synthesis.[15-17] Within the numerous reports of the synthesis of metal sulfide QDs based on S/ODE precursors, the temperature and duration reported for dissolving sulfur in ODE to prepare the precursor varies widely**.** While elemental sulfur dissolves in ODE within a few minutes at 180°C, QD synthetic procedures often describe heating the S/ODE mixture for longer than one hour, which causes a transition of the solution from colorless to bright yellow. The reactions within chalcogen-olefin mixtures have been studied extensively for decades—mostly due to the use of this chemistry in industrially important application such as rubber vulcanization and polymer synthesis[18]—but there is no study of the influence of the reaction products—namely, alkyl-polysulfur adducts—on QD nucleation and growth. The most closely related work on the role of chalcogen-olefin precursor chemistry on QD synthesis is by Bullen *et al*., who have shown that extended heating of the analogous selenium precursor Se/ODE lowers CdSe QD yields by 50% due to covalent binding of selenium and ODE.[19] Herein we describe the mechanism by which reaction of sulfur with ODE induces a change in the shape of PbS QDs synthesized from the S/ODE precursor from cubic to hexapodal by altering the ligand chemistry of the growing QD. We monitor the heating-induced structural changes in the

S/ODE precursor with ^{1}H-nuclear magnetic resonance spectroscopy (^{1}H NMR), mass spectrometry, fluorescence spectroscopy, and absorbance spectroscopy. The absolute concentrations of these adducts are small—less than 4% for the temperature ranges studied—but still dramatically alter the PbS QD growth process. Understanding the mechanism of PbS QD growth under these conditions should enable both the reproducible laboratory preparation of high quality QDs and a commercially viable synthesis of QDs using cost-effective starting materials.

EXPERIMENTAL METHODS

Materials. Sulfur flakes (99.998%), lead(II) oxide (99.999%), lead(II) acetate trihydrate (99.999%), oleylamine (70% tech. grade), 1-octadecene (90% tech. grade), oleic acid (90% tech. grade), hexadecane (99%), biphenyl (99.5%), 1-decanethiol (96%), and chloroform-d (99.8 atom% D) were purchased from Aldrich. Reagent grade acetone, chloroform, and hexanes were purchased from VWR International. All reagents and solvents were used as-received without further purification.

Preparation of the S/ODE Precursor. We prepared sulfur precursors for PbS QD synthesis by dissolving elemental sulfur in 1-octadecene solvent. We heated 100 ml ODE in a round-bottom flask to 102 °C and stirred for 1 hr under a flow of dry N_2 gas to dry. The temperature was then raised to the temperature desired for the study (180 °C to 210 °C) and 240 mg elemental sulfur flakes was swiftly added through the flask sidearm under positive N_2 pressure. Sulfur flakes completely dissolved within two to five minutes after solid addition to form an optically clear solution with a light yellow tint, which would become colorless upon cooling to room temperature. Continued heating produced a slow change in coloration to darker shades of yellow, and this coloration would persist after cooling. For heating duration studies, aliquots

were removed at specified intervals, transferred to a glass vial, and cooled using a room temperature water bath. All precursors could be effectively used for PbS QD synthesis more than two weeks following preparation when stored under ambient conditions.

Synthesis and Purification of PbS Quantum Dots. We prepared PbS QDs using a procedure modified from the one reported by Li *et al*.[17] 357 mg lead(II) oxide, 8.5 ml oleic acid, and 56 ml 1-octadecene were added to a round-bottom flask and heated to 210 °C while stirring and continuously flowing dry, N_2 gas through the vessel. Heating took approximately 1 hour, during which time the lead(II) oxide reacted with oleic acid to form a colorless, optically clear solution of lead(II) oleate. Immediately prior to reaction with the sulfur precursor, 8 ml of oleylamine was injected into the lead(II) oleate solution and the temperature allowed to rise back to 210 °C. Once the solution reached the reaction temperature of 210 °C, 8 ml of the S/ODE precursor solution was swiftly injected into the reaction vessel. The reaction solution began turning brown within 15 seconds following S/ODE injection. The reaction mixture was quenched one minute after S/ODE injection by pouring the reaction mixture into a jar of chloroform chilled in an ice water bath. We recovered the QDs by centrifuging the reaction mixture and then washed the QDs once by making them up in chloroform and crashing by adding acetone to this solution in a 3:1 (v:v) ratio of acetone:chloroform. The PbS QD product was a black precipitate that could be dispersed in either chloroform or hexanes to produce a black, optically clear colloidal QD solution.

Spectroscopic Characterization of the S/ODE Precursor. We performed ground state absorption spectroscopy of S/ODE precursor aliquots using an Agilent Technologies Cary 5000 UV-vis-NIR spectrophotometer. We acquired absorption spectra using an optical glass cuvette with a 2mm pathlength. We performed photoluminescence (PL) spectroscopy using a Horiba

Jobin Yvon Fluorolog 3 Spectrofluorometer, with emission and excitation slit widths of 5 nm and an excitation wavelength of 360 nm. All PL spectra were acquired in a 1-cm pathlength quartz cuvette; S/ODE precusors were diluted to 1% by volume in hexanes for all PL studies.

^{1}H NMR. We acquired all ^{1}H-NMR spectra of S/ODE precursor samples using a Bruker Avance III 500 MHz spectrometer and all ^{1}H-NMR spectra of PbS QDs using an Agilent DD2 600MHz spectrometer with 99.8 atom % $CDCl_3$ as a solvent. We prepared NMR samples of S/ODE precursor by adding 50 μl of the raw precursor to 1.0 ml of $CDCl_3$ with 19 mM biphenyl as an internal concentration standard. Prior to acquiring ^{1}H-NMR spectra of the PbS QD samples, we performed additional purification of the samples to remove organics not bound to the QD. We removed solvent from the QD dispersion by rotary evaporation and washed the recovered QD powder once with 5 ml of acetone followed by rotary evaporation to remove residual acetone. We made up the final samples in 1.0 ml $CDCl_3$. All signals from residual ODE—used as solvent in the QD synthesis—were gone following a single washing of the QD powder with acetone. The standard VnmrJ s2pul pulse sequence was used for all samples, except for the PbS QD samples, for which we used a two second overhead delay. Chemical shifts of all spectra were referenced to the residual $CHCl_3$ singlet at 7.26 ppm.

TEM. We performed transmission electron microscopy (TEM) on PbS QD samples using an Hitachi H-8100 TEM operated at 200 kV emission voltage. We deposited samples from chloroform onto ultrathin carbon on holey carbon/Cu TEM grids, 400 mesh (Ted Pella).

MALDI-TOF. We acquired matrix-assisted laser-desorption ionization time-of-flight mass spectra of aliquots of elemental sulfur heated in 1-octadecene at 180 °C removed at 5 and 120 minutes following sulfur addition using a Bruker Apex III MALDI. We used α-cyano-4-

hydroxycinnamic acid as the matrix material loaded to approximately 20% by mass with analyte. We acquired mass spectra in reflectron TOF mode and positive polarity.

RESULTS AND DISCUSSION

The Heating Time for the S/ODE Precursor Influences the Size and Shape of PbS QDs. We separately prepared sulfur and lead precursors by heating elemental sulfur in ODE and heating lead(II) oxide in the presence of oleic acid to form solutions of sulfur in ODE and lead(II) oleate, respectively. We then combined the lead and sulfur precursors at 210 °C under nitrogen in the presence of oleylamine to reduce sulfur *in situ* and form PbS. Over the course of heating for two hours at a temperature of 180 °C, the color of the S/ODE solution changes continuously from colorless to bright yellow. The shape and size of the PbS QDs produced from the S/ODE precursor depends on how long it is heated. For example, PbS particles prepared using a S/ODE precursor heated for two minutes at 180 °C were cubic with an average edge length of 11 ± 1 nm, whereas particles prepared using a precursor heated for two hours at 180 °C were hexapodal with an average tip-to-tip diameter of 27 ± 7 nm. The estimated hexapod volumes are between five and fifteen times larger than the mean volume for the cubes. The TEM images in **Figure 1a-d** show this transition from cubic to hexapodal QD shape as a function of the duration of S/ODE precursor heating. To understand how this seemingly small change in the precursor preparation produces such a drastic effect on the final QD shape, we analyzed the chemical changes occurring in the S/ODE precursor solution when exposed to elevated temperatures for various lengths of time.

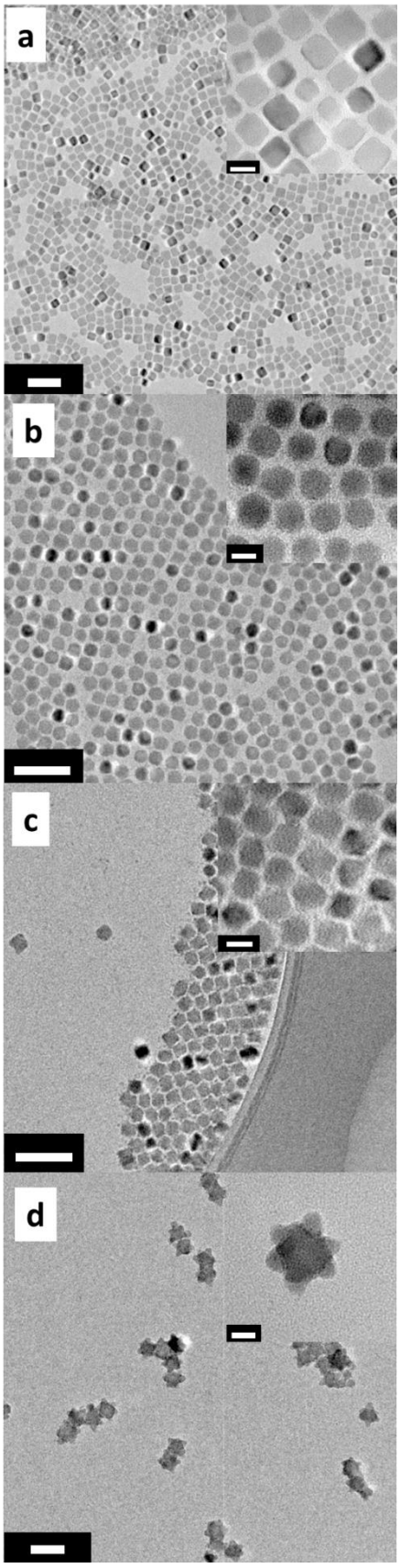

Figure 1. Transmission electron micrographs of purified PbS QDs synthesized using aliquots of sulfur heated in 1-octadecene at 180 °C under N_2 for either **a**) 5 minutes, **b**) 30 minutes, **c**) 60 minutes, or **d**) 90 minutes. The scalebar represents 50 nm for the main images and 10 nm for insets. These QDs show a shape transition from cubic to hexapodal as the heating duration of the S/ODE precursor is increased.

Colorimetric Detection of the Kinetics of the Reaction between Sulfur and ODE. The S/ODE precursor consists of elemental sulfur (i.e. cyclooctasulfur, S_8) dissolved in 1-octadecene by heating under nitrogen. While heating at 180°C, solutions of S/ODE develop a bright yellow color that persists after the solution is cooled to room temperature. The absorbance of aliquots taken at early heating times is predominantely in the ultraviolet region, but later aliquots show appreciable absorbance intensity over 400-500 nm and the emergence of a series of broad absorption peaks between 320 and 400 nm (**Figure 2a**) consistent with the observed color change. Photoluminescence (PL) spectra of aliquots of S/ODE precursor in hexanes, excited at 360 nm, show a very broad emission feature at 430 nm that grows in over time (**Figure 2b**). The broad absorbance and emission features indicate the heating produces a structurally disperse set of fluorescent species that are chemically stable for more than thirty days at ambient conditions.

We do not believe the colorimetric changes we observe are due to the formation of solvated sulfur, because when we heat elemental sulfur in hexadecane instead of ODE, the dissolution rate is very similar, but the yield of fluorescent species (λ_{em} = 430 nm) is dramatically lower in the hexadecane solutions than in the ODE solutions (**Figure S1**). This experiment reveals that the carbon-carbon double bond in ODE accelerates the formation of the stable fluorescent species.

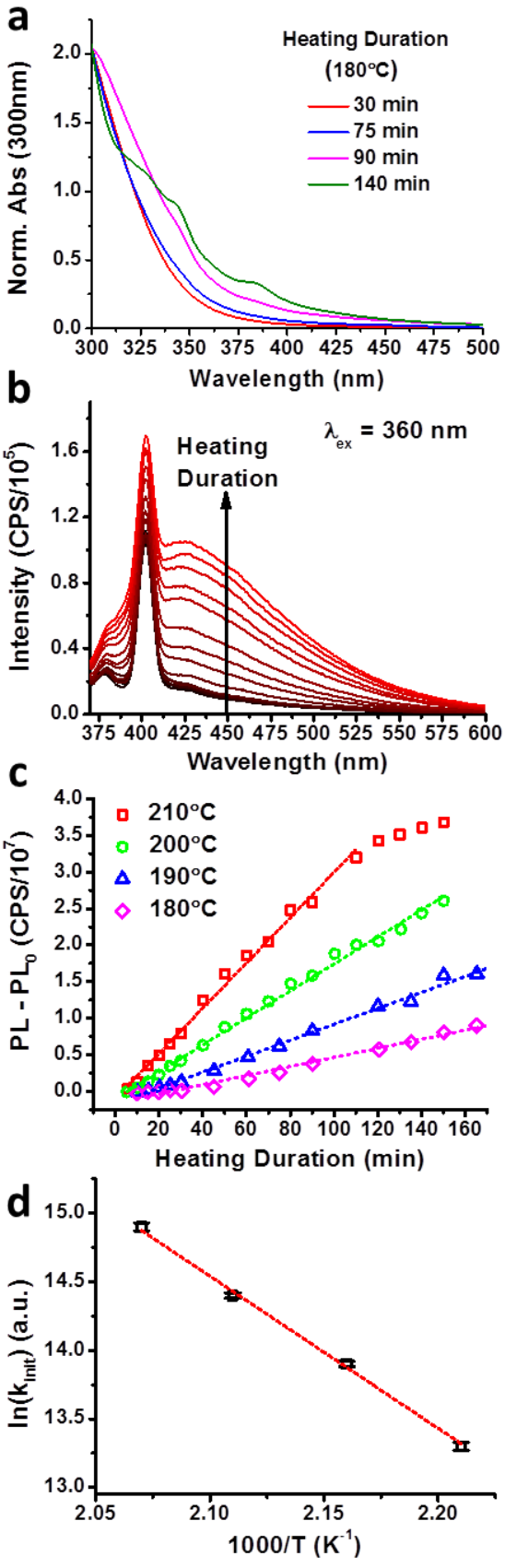

Figure 2. a) Ground state absorption spectra of S/ODE aliquots normalized to absorbance at 300nm show a shift of the absorption intensity from ultraviolet to visible wavelengths as the heating duration increases. **b)** Photoluminescence spectrum of S/ODE aliquots diluted in hexanes for a series of heating times between six and 150 minutes, and excited at 360 nm. A large, broad emission feature grows in as the S/ODE solution is heated. The sharp peak at 402nm is due to the hexanes Raman mode. **c)** Plot of the change in PL signal, integrated from λ_{em} = 370 to λ_{em} = 600 nm, of aliquots taken from an S/ODE solution heated at various temperatures, and excited at 360 nm. Linear fits of the initial rates are shown as dashed lines. **d)** Plot of the natural log of the initial PL signal growth rate versus reciprocal temperature. Error bars indicate fitting error for the linear fits in **(c)**. The Arrhenius-type behavior indicates a 92 kJ/mol activation barrier to formation of the photoluminescent species.

Figure 2c plots the change in PL signal integrated from λ_{em} = 370 to λ_{em} = 600 nm as a function of the heating time for the S/ODE solutions, for four heating temperatures: 180, 190, 200, and 210 °C. PL_0 is defined as the integrated PL for the aliquot acquired at the earliest time point; we subtract PL_0 from the integrated PL at later times to yield "PL-PL_0" in Figure 2C. This process subtracts out the Raman feature of hexanes at 402 nm. The PL intensity increases linearly with time for all temperatures, and only the PL of the samples heated at 210 °C show signs of saturation over the studied time range. **Figure 2d** shows a plot of the natural logarithm of the initial PL growth rate, obtained from linear fits of the data in **Figure 2c**, versus reciprocal temperature, and a linear fit of this data. The Arrhenius analysis yields an activation energy for the formation of the photoluminescent species of 92 kJ/mol. This activation energy is similar to the value measured for the polymerization of S_8 initiated by thiol in the presence of base.[20]

The kinetics of the colorimetric changes in S/ODE require a mechanism that forms a structurally disperse set of air-stable species, is thermally irreversible, and is accelerated by the presence of carbon-carbon double bonds. Sulfur melts undergo a discontinuous change in their viscosity at 158 °C—known as the "lambda transition"—during which the cyclooctasulfur rings that comprise elemental sulfur begin to homolytically cleave sulfur-sulfur bonds and polymerize to produce catena-sulfur, which is composed of variable-length polysulfur chains.[21] Catena-sulfur exhibits vibrationally-broadened fluorescence, but the lambda transition is generally thermoreversible. Given the acceleration of the formation of fluorescent species by the presence of a carbon-carbon double bond, we hypothesize from the colorimetric studies that the actual fluorescent species is a polysulfur-alkyl adduct formed when sulfur reacts with the double-bond of ODE. A polysulfur-alkyl adduct would retain the fluorescence of catena-sulfur while trapping sulfur in a stable, polymeric form via covalent bonding to an alkane.

^{1}H-NMR Measurement of S/ODE Reaction Products. The kinetics of colorimetric changes of S/ODE mixtures heated to 180 °C suggest a reaction between sulfur and ODE that forms fluorescent polysulfur-alkyl adducts. Previous studies of the polymerization reactions of sulfur with alkenes [18, 21] show that elemental sulfur undergoes addition chemistry with alkenes at elevated temperatures *via* either radical or ionic mechanisms (see **Scheme S**1 in the Supporting Information). Based on these mechanisms, the principal products of sulfur addition to ODE are a constitutionally disperse set of compounds with a polysulfur chain bonded to either the C1 or C2 position; in the formation of these products, the carbon-carbon double-bond either undergoes an addition reaction with sulfur or migrates to an internal position. Distinguishing between the mechanisms of S/ODE polymerization is outside the scope of the current study; we instead focus on the structure and yield of organosulfur products of the S/ODE precursor preparation on QD growth.

^{1}H-NMR spectra of aliquots taken from S/ODE solutions heated at 180 °C provide clear evidence of the structural changes associated with the reaction of sulfur and ODE. After 90 minutes of heating sulfur in ODE at 180°C, a series of new ^{1}H signals appear between 2.5 and 3.5 ppm (**Figure 3a**). **Figure 3b** shows the assignments of these features to the protons on carbons bonded to sulfur; assignments are based on ^{1}H-^{1}H Correlation Spectroscopy (**Figure S4**). Notable are –S–CH_2– groups bound to an internal carbon-carbon double-bond (product 1 in Figure 3b), which are a characteristic sign of the migration of ODE's terminal carbon-carbon double bond to an internal double bond following reaction with S_8. The distinctive peak at 2.51 ppm corresponds to –S–CH_2– bound to a tertiary carbon (product 3 in **Figure 3b**).

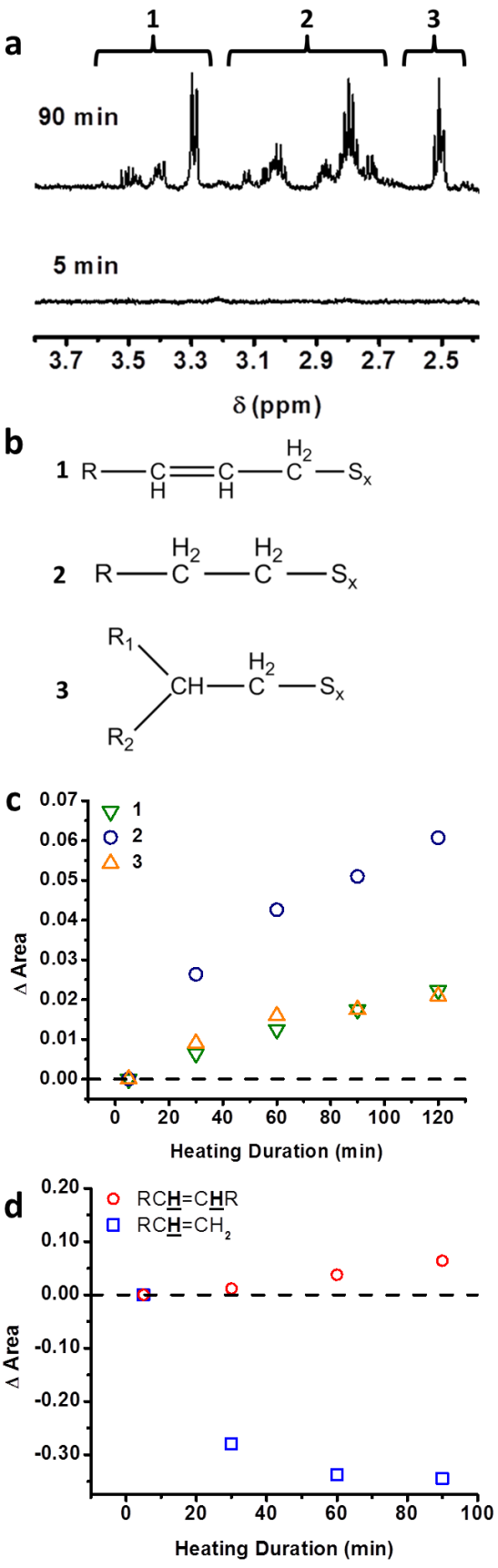

Figure 3. a) Region of the ^{1}H-NMR spectrum of S/ODE aliquots heated at 180°C for 5 minutes and 90 minutes that contain signals from protons on carbons directly bonded to sulfur. **b)** Structures corresponding to the numbered regions in **(a)**. These compounds may also take on a bridged form, where two hydrocarbon chains are linked by a variable-length sulfur chain (S_x), without measurable change in the ^{1}H NMR spectrum. **c)** The change in integrated peak area of ^{1}H-NMR peaks in **(a)** with time, for a reaction mixture of elemental sulfur and ODE heated at 180 °C. The concentrations of all three products shown in **(b)** increase with increased S/ODE heating duration. **d)** The change in integrated peak area of ^{1}H-NMR features corresponding to protons on internal (red) and terminal (blue) double bonds within the S/ODE reaction mixture after heating at 180 °C for a series of times. With increasing S/ODE heating time, the concentration of species with terminal double bonds decreases due to reduction of sulfur accompanied by either elimination of the double bond to form compounds 2 and 3, or, to a lesser degree, migration of the double bond to form compound 1 (red circles in **d** and yellow triangles in **c**).

Figure 3c shows that the integrated peak area corresponding to all organosulfur compounds (1, 2, and 3) increases with S/ODE heating time. The majority products are unsaturated, straight-chain alkanes bonded to a polysulfur chain. Branched and double-bond migration products have a lower yield.

^{1}H-NMR spectra of our samples show both an elimination of terminal double-bonds and a formation of internal double-bonds in S/ODE aliquots heated at 180 °C (**Figure 3d**); over a period of 90 minutes, the integrated peak areas associated with terminal double-bonds (δ = 5.81 ppm; δ = 4.99 ppm; δ = 4.93 ppm) all decrease by ~10% while those associated with internal double-bonds (initially present due to isomeric impurities in technical grade ODE, **Figure S2**) (δ = 5.41 ppm) increase by ~80%. Approximately ten terminal double-bonds are eliminated for every internal double-bond formed, so there is a net loss of vinyl functional groups. Following coordination of elemental sulfur to ODE's terminal double bond to form either a cation or radical intermediate (Reactions 3 and 4, Scheme S1), the intermediate can produce either: (1) a 2,3-unsaturated product following proton loss (Reactions 5 and 6, Scheme S1**)** or (2) a 1,2-disubstituted product following attack by a nucleophile. The overall loss of carbon-carbon double-bonds indicates the proton loss required for double-bond migration occurs more slowly than the nucleophilic attack required for addition to the double-bond. This result is consistent with the higher yield of saturated products (product 2 in **Figure 3b**) than 2,3-unsaturated products (product 1 in Figure 3b).

Prior work on the side products of CdS QD synthesis involving reduction of sulfur with ODE showed thiophenes to be a primary side-product of this reaction.[10] Any such compound would produce peaks between 6.7 and 7.2 ppm, but we observe no such signals in either the S/ODE precursor samples tested or the crude PbS QD product prior to purification.

If we assume each ODE molecule only forms one carbon-sulfur bond, 3% of the original ODE molecules have bound sulfur after 90 minutes of heating at 180 °C. Matrix-assisted laser-desorption time-of-flight mass spectroscopy of S/ODE shows the formation of compounds at m/z = 282 and 530 during heating. The lighter fragment is consistent with a single sulfur atom bound to a single ODE molecule, and the heavier fragment is consistent with two ODE molecules bridged by a sulfur atom (**Figure S5**). Higher molecular weight fragments were not observed, so the principal S/ODE reaction products of interest are either: (1) $C_{17}H_{34}–CH_2–S_x$ or (2) $C_{17}H_{34}–CH_2–S_x–CH_2–C_{17}H_{34}$, where x is an integer. ODE heated for two hours at 210 °C without sulfur present showed no change in integrated vinyl or aliphatic proton signals (**Figure S3**).

^{1}H-NMR confirms the presence of products of types 1, 2, and 3 in Figure 3b from reaction of elemental sulfur with ODE. The reaction of sulfur with ODE therefore produces multiple new stable species that able to coordinate to the QD surface.

Mechanism by which S/ODE Polymerization Influences the Growth of PbS QDs. For all temperatures studied, elemental sulfur flakes readily dissolved within five minutes of addition to hot ODE. In contrast, the S/ODE reactions progress over a timescale of hours (**Figures 2, 3**). We therefore conclude that the dependence of the growth of PbS QDs on the heating time of the S/ODE precursor (**Figure 1**) is not attributable to incomplete dissolution of sulfur at short heating durations. Three possible mechanisms by which ODE reduction of sulfur affects the PbS QD synthesis are: (1) loss of sulfur as H_2S gas, (2) decreased oleylamine reduction activity, and (3) coordination of polymerization products to the growing QD surface. Mechanisms (1) and (2) render the S/ODE solution a less effective source of amine-reducible sulfur and mechanism (3) alters the QD growth process via *in situ* generation of organosulfur ligands.

We tested mechanisms (1) and (2) by quantifying the evolved H_2S gas both during the dissolution of sulfur in ODE to form the S/ODE precursor, and during the reaction of S/ODE with oleylamine (**Figures S6 and S7**). Even when heated at 210°C, the S/ODE solution only loses 0.5% of its total sulfur content as H_2S gas over the first two hours of heating. The yield of H_2S produced by reacting S/ODE with oleylamine is not measurably affected by the heating duration of the S/ODE precursor prior to reaction. We conclude that for the S/ODE preparation temperatures and durations employed in this study, neither the amount of available sulfur nor its reactivity with oleylamine significantly affect the yield of the reduced sulfur species that form PbS. We also checked whether the QD synthesis was affected at all by trace water by applying vacuum to the lead(II) oleate and oleylamine in ODE solution at 80°C, but we observed no change in PbS QD shape or size following more rigorous water exclusion (**Figure S8**). Elucidating water's complex role in QD growth, which may include altering the number of bound oleate ligands and participating in the reduction of elemental sulfur by amines, is outside the role of the current study. As such we have not attempted to quantify the amount of remaining water; the application of vacuum to the precursor solution shows the reaction is insensitive to the variations in water concentration commonly encountered in laboratory QD synthesis.

If the *in situ* creation of polysulfur-alkyl adducts affects the PbS QDs' shape by binding to the growing QD (mechanism 3), we should observe changes in the types of ligands present on the final, purified particles. We prepared PbS QDs according to a published method by injecting S/ODE precursor into a solution of lead (II) oleate in ODE at 210 °C with oleylamine as an *in situ* sulfur reducing agent.[17] We repeated the PbS QD synthesis using S/ODE precursors prepared by heating sulfur in ODE for 5, 30, 60, and 90 min at 180 °C and washed the recovered QD powder with acetone to remove residual ODE. All QD workup was performed in $CHCl_3$.

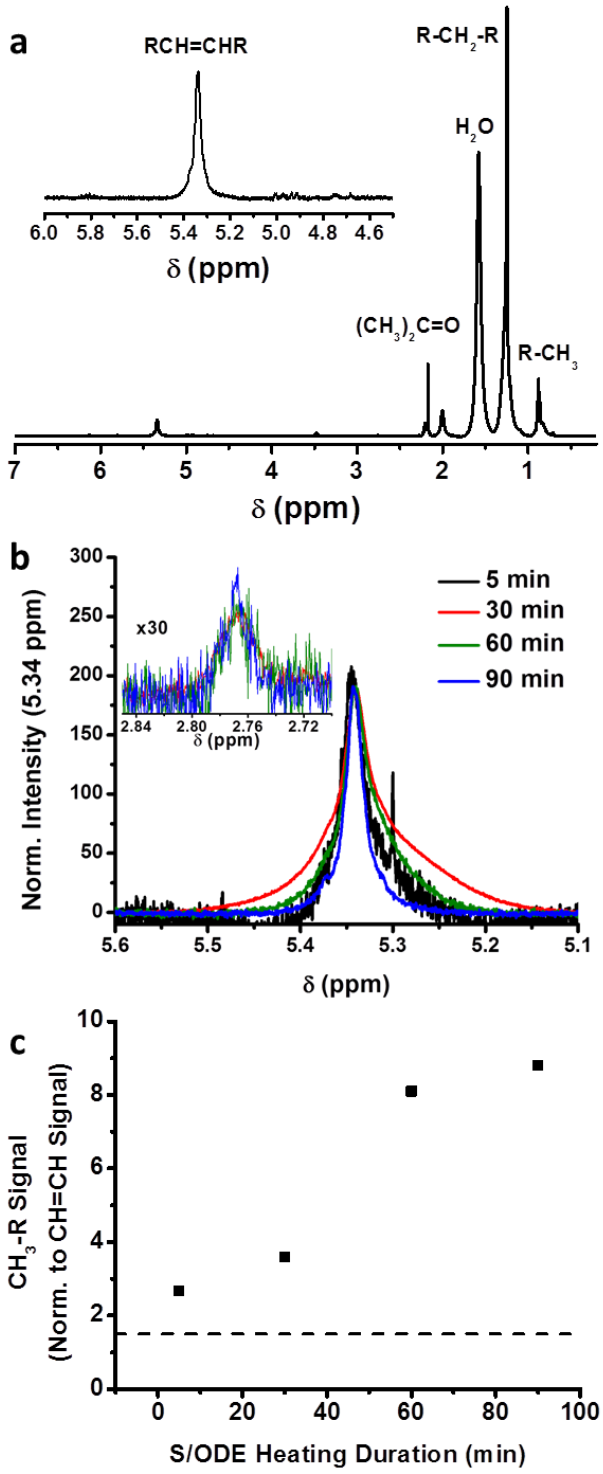

Figure 4. (a) Representative ^{1}H-NMR spectrum of purified PbS QDs in $CDCl_3$ synthesized using sulfur heated in ODE for 30 min; a zoom-in on the vinyl region is shown in the inset. The relevant signals associated with protons on internal carbon-carbon double-bonds and terminal methyl groups are indicated along with residual acetone and H_2O peaks. The broad, intense peak at 1.27 ppm comes from protons on alkyl carbons at least one carbon removed from any functional groups. **(b)** Vinyl and organosulfur (inset) regions of ^{1}H NMR spectra of samples of PbS QDs synthesized using S/ODE precursors prepared by heating at 180°C for 5, 30, 60, or 90 minutes. The intensity of all spectra have been scaled to make their intensities at 5.34 ppm equal to more easily compare their linewidths. All samples except for the five minute sample include a broad signal from protons on the carbon alpha to the sulfur at 2.77 ppm (inset). **(c)** Ratio of signal from CH_3-R protons relative to CH=CH protons (determined by integrated peak areas) for PbS QDs synthesized using a sulfur precursor prepared by heating sulfur in ODE for the indicated duration. The dashed line indicates the expected CH_3-R:CH=CH signal ratio if the only ligand bound to the QDs were oleate.

Figure 4a shows a representative ^{1}H-NMR spectrum of purified PbS QDs; the peaks corresponding to hydrogens on an internal carbon-carbon double bond (δ = 5.34 ppm) and on a terminal methyl group (δ = 0.88 ppm) are highlighted. The vinyl peak at 5.34 ppm is broader than that of free oleic acid, which is a clear doublet of triplets, and the linewidth of this signal varies from sample to sample, so we know that at least a portion of the oleate in the sample is bound to the QD at any given time. We also observe a weak feature at 2.77 ppm (**Figure 4b, inset**) that, based on comparison with spectra of 1-decanethiolate bound to PbS QDs (**Figure S9**), we assign to an organosulfur species undergoing exchange with the QD surface. The signal at 2.77 ppm is most intense for QDs prepared using a S/ODE precursor heated at 180°C for 90 minutes and indistinguishable from noise for QDs prepared using the S/ODE precursor heated for 5 minutes. We do not attempt to analyze this signal quantitatively because the integration of signals from these ligands becomes more unreliable as the binding constant of the ligand increases and the signal broadens.

Figure 4c plots the ratio of integrated peak area associated with protons on CH_3-R groups (δ = 0.88 ppm) to the integrated peak area associated with protons on R-CH=CH-R groups (δ = 5.34 ppm). The ratio of methyl-to-vinyl protons increases with S/ODE precursor heating duration. There are two conclusions we draw from this data. (i) Oleate, which binds to Pb^{2+} on the surface of the QDs, cannot be the only ligand binding to the QD surface. Oleate contains one CH_3-R and one R-CH=CH-R group, and we should observe their integrated ^{1}H-NMR signal ratio to be 1.5:1 (as indicated by the dotted line in **Figure 4c**) if oleate is the only ligand bound to the QD surface. At least one other structurally distinct ligand must be present to account for this discrepancy. We believe that the additional ligands are organosulfur compounds of types 1, 2, and 3 (**Figure 3b**) produced during the S/ODE reaction; these compounds remain on the QD

surface after purification. (ii) The ratio of organosulfur molecules to oleate ligands in the sample, as indicated by the proton signal ratio in **Figure 4c**, increases with the heating duration of the S/ODE precursor. The change in shape of the QDs (from cubic and hexapodal, **Figure 1**) is correlated with the molar ratio of organosulfur species to oleate.

Previous studies of anisotropic PbS nanoparticle synthesis have shown that ligand chemistry can control PbS QD shape by controlling the differential rates of growth along <100> and <111> crystal faces[23-26]. Preferential growth along <100> faces leads to hexapods while preferential growth along <111> faces leads to cubes or octapods. Density functional calculations of the binding isotherms of oleate ions to PbSe <100> and <111> faces show these faces to be in a competitive equilibrium based on the concentration of oleate ions in solution, and <100> faces lose coverage more rapidly than <111> faces as the oleate ion concentration decreases. These calculations predict a transition from cubic to octahedral QD growth as oleate ion concentration is decreased, which is consistent with experiment.[27-28] Any organosulfur species produced by the S/ODE reaction would presumably bind through the sulfur in a binding motif similar to a thiol. Like oleate, thiols preferentially bind to <111> faces because they adopt a μ^3-Pb_3-SR bridging mode where they can bind to three lead atoms; thiol addition favors <100> face growth.[24] In fact, 1-dodecanethiol has been used to synthesize PbS hexapods both via the thermal decomposition of a molecular PbS precursor and via the direct reaction of the thiol with lead(II) acetate.[29-30]

The partitioning of any ligand between the <100> and <111> faces is controlled by: (i) the relative binding energy of the ligand on the faces and (ii) the concentration of the ligand, with lower concentrations favoring coverage of the face with the higher binding energy. The concentration of organosulfur compounds produced during S/ODE heating is less than 10% of the concentration of oleate molecules, so the adducts should preferentially bind to <111> binding

sites. These organosulfur compounds also may have a higher molecular weight than the oleate ligands because they are the result of a polymerization process with 1-octadecene. This combination of a binding preference for <111> faces and high molecular weight makes these compounds highly effective at retarding growth at the <111> faces, such that preferential growth of the <100> faces results in formation of QDs with octahedral symmetry (i.e. hexapods). This prediction is consistent with the observed results: as the heating duration of the S/ODE precursor is extended and more of the organosulfur products are formed, the shape of QDs changes from cubic (i.e. primarily <111>-face growth) to hexapodal (i.e. primarily <100>-face growth).

CONCLUSIONS

We have described the variation of PbS QD shape from cubic to hexapodal caused by increasing the heating time of the S/ODE precursor from five minutes to two hours at 180°C, which is a typical temperature and range of heating durations found in published PbS QD syntheses. ^{1}H-NMR spectra indicate that extended heating of S/ODE causes sulfur and ODE to react and produce a series of organosulfur products. This reaction does not measurably affect the reactivity of the S/ODE precursor with lead oleate; however, NMR spectra of purified PbS QDs indicated that the organosulfur products of this reaction bind to the QD surface, even after the QDs are purified by precipitation and washing with acetone. The creation of organosulfur ligands during S/ODE heating provides a mechanism for QD shape control: the binding of these ligands to the growing QD induces a preferential growth at the <100> faces, and therefore a hexapodal geometry for the particles.

Techniques to produce PbS particles of various shapes – often using S/ODE precursors – are the focus of numerous reports.[17, 23, 25-26, 29-38] Since the timescale of reaction between sulfur and

ODE is significantly longer than the timescale of sulfur dissolution—hours instead of minutes—S/ODE can be made a much more reliable precursor by reducing the temperature and duration of the sulfur dissolution step. Additionally, any metal sulfide QD synthesis using elemental sulfur heated to high temperatures should take steps to reduce the *in situ* yield of organosulfur byproducts by avoiding olefinic solvents.

Our present work on the S/ODE precursor has focused solely on the effects of organosulfur compounds on the growth stage of QD synthesis. Further work will investigate the role of these compounds in the much faster nucleation process and its influence on the QD product.

Supporting Information Available. Additional experimental methods, pathways for polymerization of sulfur and ODE, additional ^{1}H NMR spectra of ODE and crude PbS product, COSY NMR and MALDI-TOF spectra of the S/ODE precursor, measurement of sulfur loss as H_2S, measurement of S/ODE reactivity with ODE, effect of residual water on the synthesis, thiol titration of PbS QDs, and Figures S1-S10. This information is available free of charge via the Internet at http://pubs.acs.org/.

Acknowledgements. This project was funded by the National Science Foundation through the Northwestern Materials Research Science and Engineering Center (grant **DMR-1121262).** The authors acknowledge the EPIC facility of the NUANCE Center at Northwestern University where electron microscopy studies were performed and the IMSERC facility at Northwestern University for the use of nuclear magnetic resonance and mass spectrometry facilities.

REFERENCES

(1) Yu, W. W.; Peng, X., Formation of High-Quality CdS and Other II-VI Semiconductor Nanocrystals in Noncoordinating Solvents: Tunable Reactivity of Monomers. *Angew. Chem. Int. Ed.* **2002,** *41* (13), 2368-2371.

(2) Chon, J. W. M.; Gu, M.; Bullen, C.; Mulvaney, P., Three-photon excited band edge and trap emission of CdS semiconductor nanocrystals. *Appl. Phys. Lett.* **2004,** *84* (22), 4472 - 4474.

(3) Embden, J. v.; Jasieniak, J.; Mulvaney, P., Mapping the Optical Properties of CdSe/CdS Heterostructure Nanocrystals: The Effects of Core Size and Shell Thickness. *J. Am. Chem. Soc.* **2009,** *131*, 14299 - 14309.

(4) Gomez, D. E.; Pastoriza-Santos, I.; Mulvaney, P., Tunable Whispering Gallery Mode Emission from Quantum-Dot-Doped Microspheres. *Small* **2005,** *1* (2), 238 - 241.

(5) Guo, W.; Li, J. J.; Wang, Y. A.; Peng, X., Luminescent CdSe/CdS Core/Shell Nanocrystalsin Dendron Boxes: Superior Chemical, Photochemical and Thermal Stability. *J. Am. Chem. Soc.* **2003,** *125*, 3901 - 3909.

(6) Huang, L.; Wang, X.; Yang, J.; Liu, G.; Han, J.; Li, C., Dual Cocatalysts Loaded Type I CdS/ZnS Core/Shell Nanocrystals as Effective and Stable Photocatalysts for H_2 Evolution. *J. Phys. Chem. C* **2013,** *117*, 11584 - 11591.

(7) Li, J. J.; Wang, Y. A.; Guo, W.; Keay, J. C.; Mishima, T. D.; Johnson, M. B.; Peng, X., Large-Scale Synthesis of Nearly Monodisperse CdSe/CdS Core/Shell nanocrystals Using Air-Stable Reagents via Successive Ion Layer Adsorption and Reaction. *J. Am. Chem. Soc.* **2003,** *125*, 12567 - 12575.

(8) Li, X.; Bullen, C.; Chon, J. W. M.; Evans, R. A.; Gu, M., Two-photon-induced three-dimensional optical data storage in CdS quantum-dot doped photopolymer. *Appl. Phys. Lett.* **2007,** *90* (16), 161116-1 - 161116-3.

(9) Li, Y.; Liu, E. C. Y.; Pickett, N.; Skabara, P. J.; Cummins, S. S.; Ryley, S.; Sutherland, A. J.; O'Brien, P., Synthesis and characterization of CdS quantum dots in polystyrene microbeads. *J. Mater. Chem.* **2004,** *15*, 1238 - 1243.

(10) Li, Z.; Li, Y.; Xie, R.; Grisham, S. Y.; Peng, X., Correlation of CdS Nanocrystal Formation with Elemental Sulfur Activation and Its Implication in Synthetic Development. *J. Am. Chem. Soc.* **2011,** *133*, 17248-17256.

(11) Protiere, M.; Reiss, P., Facile synthesis of monodisperse ZnS capped CdS nanocrystals exhibiting efficient blue emission. *Nanoscale Res. Lett.* **2006,** *1*, 62 - 67.

(12) Swafford, L. A.; Weigand, L. A.; II, M. J. B.; McBride, J. R.; Rapaport, J. L.; Watt, T. L.; Dixit, S. K.; Feldman, L. C.; Rosenthal, S. J., Homogeneously Alloyed CdS_xSe_{1-x} Nanocrystals:

Synthesis, Characterization, and Composition/Size-Dependent Band Gap. *J. Am. Chem. Soc.* **2006,** *128*, 12299 - 12306.

(13) Wang, C.; Zhang, H.; Zhang, J.; Li, M.; Han, K.; Yang, B., The influence of oxygen on the fluorescence enhancement of fatty-acid-capped CdS nanocrystals. *J. Colloid Interface Sci.* **2006,** *294*, 104 - 108.

(14) Yu, Z.; Li, J.; O'Connor, D. B.; Wang, L.-W.; Barbara, P. F., Large Resonant Stokes Shift in CdS Nanocrystals. *J. Phys. Chem. B* **2003,** *107*, 5670 - 5674.

(15) Acharya, K. P.; Hewa-Kasakarage, N. N.; Alabi, T. R.; Nemitz, I.; Khon, E.; Ullrich, B.; Anzenbacher, P.; Zamkov, M., Synthesis of PbS/TiO_2 Colloidal Heterostructures for Photovoltaic Applications. *J. Phys. Chem. C* **2010,** *114*, 12496 - 12504.

(16) Liu, T.-Y.; Li, M.; Ouyang, J.; Zaman, M. B.; Wang, R.; Wu, X.; Yeh, C.-S.; Lin, Q.; Yang, B.; Yu, K., Non-Injection and Low-Temperature Approach to Colloidal Photoluminescent PbS Nanocrystals with Narrow Bandwidth. *J. Phys. Chem. C* **2009,** *113* (2301 - 2308).

(17) Li, H.; Chen, D.; Li, L.; Tang, F.; Zhang, L.; Ren, J., Size- and shape-controlled synthesis of PbSe and PbS nanocrystals *via* a facile method. *CrystEngComm* **2010,** *12*, 1127 - 1133.

(18) Pryor, W. A., *Mechanisms of Sulfur Reactions*. McGraw-Hill: New York, 1962.

(19) Bullen, C.; Embden, J. v.; Jasieniak, J.; Cosgriff, J. E.; Mulder, R. J.; Rizzardo, E.; Gu, M.; Raston, C. L., High Activity Phosphine-Free Selenium Precursor Solution for Semiconductor Nanocrystal Growth. *Chem. Mater.* **2010,** *22*, 4135 - 4143.

(20) Bordoloi, B. K.; Pearce, E. M., Kinetics of the Base-Catalyzed Reactions of Cyclooctameric and Catenapolymeric Sulfur with Dithiol. *J. Appl. Polym. Sci.* **1979,** *23*, 2757-2761.

(21) Meyer, B., Elemental Sulfur. *Chem. Rev.* **1976,** *76* (3), 367-388.

(22) Thomson, J. W.; Nagashima, K.; Macdonald, P. M.; Ozin, G. A., From Sulfur-Amine Solutions to Metal Sulfide Nanocrystals: Peering into the Oleylamine-Sulfur Black Box. *J. Am. Chem. Soc.* **2011,** *133*, 5036 - 5041.

(23) Ma, Y.; Qi, L.; Ma, J.; Cheng, H., Hierarchical, Star-Shapd PbS Crystals Formed by a Simple Solution Route. *Cryst. Growth Des.* **2004,** *4* (2), 351-354.

(24) Jun, Y.-w.; Lee, J.-H.; Choi, J.-s.; Cheon, J., Symmetry-Controlled Colloidal Nanocrystals: Nonhydrolytic Chemical Synthesis and Shape Determining Parameters. *J. Phys. Chem. B* **2005,** *109*, 14795 - 14806.

(25) Zhao, N.; Qi, L., Low-Temperature Synthesis of Star-Shaped PbS Nanocrystals in Aqueous Solutions of Mixed Cationic/Anionic Surfactants. *Adv. Mater.* **2006,** *18*, 359-362.

(26) Shao, S.; Zhang, G.; Zhou, H.; Sun, P.; Yuan, Z.; Li, B.; Ding, D.; Chen, T., Morphological evolution of PbS crystals under the control of L-lysine at different pH values: The ionization effect of the amino acid. *Solid State Sciences* **2007,** *9*, 725-731.

(27) Argeri, M.; Fraccarollo, A.; Grassi, F.; Marchese, L.; Cossi, M., Density Functional Theory Modeling of PbSe Nanoclusters: Effect of Surface Passivation on Shape and Composition. *J. Phys. Chem. C* **2011,** *115*, 11382-11389.

(28) Bealing, C. R.; Baumgardner, W. J.; Choi, J. J.; Hanrath, T.; Hennig, R. G., Predicting Nanocrystal Shape through Consideration of Surface-Ligand Interactions. *ACS Nano* **2012,** *6* (3), 2118 - 2127.

(29) Lee, S.-M.; Jun, Y.-w.; Cho, S.-N.; Cheon, J., Single-Crystalline Star-Shaped Nanocrystals and Their Evolution: Programming the Geometry of Nano-Building Block. *J. Am. Chem. Soc.* **2002,** *124*, 11244-11245.

(30) Wang, Y.; Tang, A.; Li, K.; Yang, C.; Wang, M.; Ye, H.; Hou, Y.; Teng, F., Shape-Controlled Synthesis of PbS Nanocrystals via a Simple One-Step Process. *Langmuir* **2012,** *28*, 16436-16443.

(31) Zhang, W.; Yang, Q.; Xu, L.; Yu, W.; Qian, Y., Growth of PbS crystals from nanocubes to eight-horn-shaped dendrites through a complex synthetic route. *Mater. Lett.* **2005,** *59*, 3383-3388.

(32) Zhou, G.; Lu, M.; Xiu, Z.; Wang, Z.; Wang, S.; Zhang, H.; Zhou, Y.; Wang, S., Controlled Synthesis of High-Quality PbS Star-Shaped Dendrites, Multipods, Truncated Nanocubes, and Nanocubes and Their Shape Evolution Process. *J. Phys. Chem. B* **2006,** *110*, 6543-6548.

(33) Quan, Z.; Li, C.; Zhang, X.; Yang, J.; Yang, P.; Zhang, C.; Lin, J., Polyol-Mediated Synthesis of PbS Crystals: Shape Evolution and Growth Mechanism. *Cryst. Growth Des.* **2008,** *8* (7), 2384-2392.

(34) Wang, N.; Cao, X.; Guo, L.; Yang, S.; Wu, Z., Facile Synthesis of PbS Truncated Octahedron Crystals with High Symmetry and Their Large-Scale Assembly into Regular Patterns by a Simple Solution Route. *ACS Nano* **2008,** *2* (2), 184-190.

(35) Ding, B.; Shi, M.; Chen, F.; Zhou, R.; Deng, M.; Wang, M.; Chen, H., Shape-controlled syntheses of PbS submicro-/nano-crystals via hydrothermal method. *J. Cryst. Growth* **2009,** *311*, 1533-1538.

(36) Wang, Y.; Dai, Q.; Yang, X.; Zou, B.; Li, D.; Liu, B.; Hu, M. Z.; Zou, G., A facile approach to PbS nanoflowers and their shape-tunable single crystal hollow nanostructures: Morphology evolution. *CrystEngComm* **2011,** *13*, 199-203.

(37) Phuruangrat, A.; Thongtem, T.; Kuntalue, B.; Thongtem, S., Characterization of cubic and star-shaped dendritic PbS structures synthesized by a solvothermal method. *Mater. Lett.* **2012,** *81*, 55-58.

(38) Wang, Y.; Yang, X.; Xiao, G.; Zhou, B.; Liu, B.; Zou, G.; Zou, B., Shape-controlled synthesis of PbS nanostructures from -20 to 240C: the competitive process between growth kinetics and thermodynamics. *CrystEngComm* **2013,** *15*, 5496-5505.

TOC Figure